Universitatea
Transilvania
din Brașov

ȘCOALA DOCTORALĂ INTERDISCIPLINARĂ

Facultatea: Inginerie Electrică și Știința Calculatoarelor

Cosmin-Ioan Niță

Personalized, High Performance, Hemodynamics Simulation of Human Circulatory System, using the Lattice-Boltzmann method

ABSTRACT

Conducător științific

Prof. dr. ing. Florin-Dumitru MOLDOVEANU

BRAȘOV, 2020

Universitatea
Transilvania
din Brașov

D-lui (D-nei) .....

Componența

Comisiei de doctorat

Numită prin ordinul Rectorului Universității Transilvania din Brașov

Nr. ..... din .....

Prof. dr. ing. MORARU Sorin-Aurel	Președinte, Universitatea Transilvania din Brașov
Prof. dr. ing. MOLDOVEANU Florin-Dumitru	Conducător științific, Universitatea Transilvania din Brașov
Prof. dr. ing. MICLEA Liviu	Referent Oficial, Universitatea Tehnică din Cluj-Napoca
Prof. dr. ing. POPESCU Dumitru	Referent Oficial, Universitatea Politehnica din București
Prof. dr. ing. ITU Lucian-Mihai	Referent Oficial, Universitatea Transilvania din Brașov

Data, ora şi locul susținerii publice a tezei de doctorat: ....., ora ....., sala .....

Eventualele aprecieri sau observații asupra conținutului lucrării vor fi transmise electronic, în timp util, pe adresa nita.cosmin.ioan@unitbv.ro

Totodată, vă invităm să luați parte la şedința publică de susținere a tezei de doctorat.

Vă mulțumim.

Contents

1. Introduction

Cardiovascular diseases (CVD) are the leading cause of death worldwide. Currently CVDs causes 3.9 million deaths in EU accounting for 37% of all deaths. Every year 11.3 million new cases are diagnosed. It is estimated that CVD treatment costs EU economy about 210 million euros per year. The incidence of CVDs is estimated to further increase in the following decades. The most significant cause for this increase is population aging, however there are multiple known risk factors e.g. obesity and diabetes, which are also predicted to increase [5].

A significant challenge with treating CVDs is deciding on the right treatment, in fact most of the cost on treating a CVD patient results from either over or undertreatment which is caused by the lack of detailed insight on the patient. Deciding on the severity and treatment planning typically requires invasive measurements which are not just expensive but also potentially dangerous e.g. intracardiac catheterization. Furthermore, there is often need for parameters which are not available even through measurement e.g. shear stress.

A promising solution, which has attracted a lot of interest in the last decade, consist on employing numerical tools from the engineering field for modeling physiological processes and obtaining unprecedented insight with immense value for a clinician. There are multiple scenarios where such tools can be employed, for instance they can be used as an augmentation layer on top of existing diagnosis tools. In this case, a numerical simulation is performed using existing patient data as input for providing a more complete picture of the underlying physiological process. On other words, this technique can be seen as an interpolation. More specifically, through existing measurement techniques a discrete picture of the patient is obtained containing a limited amount of information. For instance, through imaging one can obtain positions and shapes of blood vessels, motion, information about the underlying tissue, etc. However, "in between" information can only be marginally obtained, e.g. flow related quantities (pressures, velocities) or other mechanical tissue properties (strains, elastic properties, etc). Through a numerical simulation based on fluid and structural mechanics, and using existing imaging information as input, one can obtain a more complete picture containing physics-based "interpolated" information.

A second scenario where such methods can be employed consist on performing an "extrapolation". In the first scenario, a numerical simulation can provide insight into the physiological process related to the patient and associated disease. In the second scenario, a numerical simulation is used to see beyond the current state of the patient and explore changes in multiple variables. More specifically a clinician can explore different treatment options and see the outcome instantly, before deciding the actual treatment. For example one can perform a virtual implantation of a mechanical device e.g. a stent or heart valve and then see the resulting effect on blood flow.

1.1 Blood flow modeling methodologies

Blood flow is a highly coupled and non-linear system both at microscopic and macroscopic level. It interacts with both the cells in its composition and with the surrounding tissue i.e. the vessel walls. Taking into account the effect of these interactions requires more than a standard CFD model. To this extent, there are various methodologies proposed in literature which able to capture different spectra of the underlying physiological process.

The first immediate class of modeling methodologies consists on approximating the flow with the fluid component only and ignoring the other effects. Although may be considered naive, this approach is the most widely accepted in literature. An important advantage is that existing CFD implementations e.g. mature products used in the engineering field, can be directly employed. The only remaining difficulty in this case is setting the boundary conditions, this require information which is often not available and must be approximated, for example inlet flowrate, outflow pressure, fluid viscosity, etc.

Another class of methods consist on taking into account both the fluid and solid components, in this case a fluid-solid interaction (FSI) simulation is required. Depending on how the interaction between fluid and solid is performed, there are two classes that can be distinguished: one-way and two-way FSI. In the case of two-way FSI, the coupling between fluid and solid is fully performed, more specifically the blood flow displaces the surrounding vessel wall due to pressure and strain forces, whereas the vessel wall movement also displaces the fluid. In the case on one-way FSI, the coupling is only partially performed: forces generated by the fluid flow are no longer enforced on the solid side. In this case, the solid wall is moved externally.

There are multiple methods for performing CFD simulations. The classic approach is based on continuum mechanics and requires dicretization of underlying flow equations, typically Navier-Stokes equations. Depending on discretization technique, there are multiple methods that can be derived e.g. finite element method (FEM), finite volume method (FVM), finite differences method (FDM), etc. Although these can be considered standard approaches and have been used extensively so far, there is another method that recently emerged and generated interest: the Lattice-Boltzmann Method (LBM). Unlike classic methods which are based on Newtonian mechanics, LBM is based on a statistical approach describing the fluid at a molecular level. Although its implementation is fundamentally different, it can be theoretically shown through Chapman-Enskog expansion [21] that it approximates the Navier-Stokes equations up to second order. The main advantage of LBM, which makes it attractive to blood flow computations is the numerical implementation. Compared to classic methods, LBM is inherently a parallel algorithm which can benefit from parallel hardware and deliver unprecedented performance. Furthermore LBM is also suited for performing FSI simulations as it can be much simpler to incorporate moving boundaries in its implementation.

1.2 Overview of present work

This thesis is structured in 6 chapters. The first chapter, Introduction, contains an overview on what are the main challenges diagnosing and treating CVDs, and how numerical modeling of the cardiovascular system can help. Also an overview on the existing methodologies for performing such simulations is provided. Finally a description of what are the difficulties and limitations of blood flow simulations and what are the existing solutions is

presented.

In the second chapter, Lattice Boltzmann method for hemodynamics simulation, an introduction of the Lattice-Boltzmann method (LBM) is provided. It contains a brief theoretical background on LBM followed by a practical description on how to achieve a numerical implementation.

In the third chapter, Fluid-Structure Interaction simulation using Lattice-Boltzmann Method, the scenario where fluid interaction with surrounding tissue is discussed. In this chapter a methodology for performing one-way Fluid-Structure interaction (FSI) is propised, i.e. where the motion of the wall boundaries is imposed. A Graphics Processing Unit (GPU) accelerated Lattice-Boltzmann Method (LBM) implementation is proposed along with an efficient workflow for embedding the moving geometry, given as a set of polygonal meshes, in the LBM computation. The proposed method is first validated in a synthetic experiment: a vessel which is periodically expanding and contracting. Next, the evaluation focuses on the 3D Peristaltic flow problem: a fluid flows inside a flexible tube, where a periodic wave-like deformation produces a fluid motion along the centerline of the tube. Different geometry configurations are used and results are compared against previously published solutions. The efficient approach leads to an average execution time of approx. one hour per computation, whereas 50% of it is required for the geometry update operations. Finally, the effect of changing the Reynolds number on the flow streamlines is analyzed: the flow regime is significantly affected by the Reynolds number. Furthermore an efficient solution for performing solid voxelization and dealing with unstructured anatomical geometries is proposed. Solid voxelization represents the process of transforming an unstructured polygonal mesh into a voxel representation by associating each polygon of a mesh with the cells in the voxel grid. A novel approach for the voxelization of solid objects is introduced, designed for Graphics Processing Units (GPU). The method is based on a heuristic approach that computes an approximate distance field instead of using mesh surface normals or exact point-to-triangle distances. Two main steps are required: voxel marking and distance field computation. In the first step, each voxel is marked based on its location relative to the mesh (inside, outside of the domain or on its boundary), and, during the second step, a signed distance field is computed. Experiments focused on meshes encountered in medical imaging applications: a left ventricle and a coronary artery. The proposed method is found to be exceptionally robust as it is able to handle meshes with severe defects such as self intersections and holes. The GPU based implementation is on average 20 times faster than the multi-core CPU based implementation.

Next, two-way fluid structure interaction simulations are also discussed. A coupling strategy with a finite-element based numerical model for the surrounding tissue is discussed. Furthermore, one of the major difficulties on performing a coupled fluid-solid simulation is discussed: numerical instability. A stability analysis study is performed for a simplified scenario resulting in clear stability boundary for model parameters. Finally some experiments with real patient data are performed along with a comparison between flow velocities obtained from simulations and from 4D MRI imaging.

The 4th chapter, Non invasive hemodynamic assessment of cerebral aneurysms, a specific use case for blood flow simulation is discussed and an efficient methodology is proposed. In recent years, Computational Fluid Dynamics (CFD) has become a valuable tool for investigating hemodynamics in cerebral aneurysms. CFD provides flow-related quantities, which have been shown to have a potential impact on aneurysm growth and risk of rupture. However, the adoption of CFD tools in clinical settings is currently limited by the high computational cost and the engineering expertise required for employing these tools, e.g.

for mesh generation, appropriate choice of spatial and temporal resolution, and of boundary conditions. Herein these challenges are addressed by introducing a practical and robust methodology, focusing on computational performance and minimizing user interaction through automated parameter selection. A fully automated pipeline is proposed, that covers the steps from patient-specific anatomical model to results, based on a fast, GPU accelerated, CFD solver and a parameter selection methodology. A reduced order model was used to compute initial estimates of the spatial and temporal resolution and an iterative approach that further adjusts the resolution during the simulation without user interaction. The pipeline and the solver are validated based on previously published results, and by comparing the results obtained for 20 cerebral aneurysm cases with those generated by a state-of-the-art commercial solver (Ansys CFX, Canonsburg PA). Specifically, the automatically selected spatial and temporal resolution leads to results which closely agree with the state-of-the-art with an average relative difference of 2%. Due to the GPU based parallelization, simulations are computationally efficient, with a median computation time of 40 minutes per simulation.

The 5th chapter, Non invasive hemodynamic assessment of aortic coarctation, presents another use case where blood flow modeling can be used for performing non-invasive diagnosis: Aortic coarctation. Coarctation of Aorta (CoA) is a congenital disease consisting of a narrowing that obstructs the systemic blood flow. Diagnosis and treatment planning of CoA relies not only geometric properties of the vessel, but also on the trans-CoA pressure drop which is typically measured invasively using catherization. Herein, a framework for automatically and robustly personalizing aortic hemodynamic computations is proposed, for the assessment of pre- and post-intervention CoA patients. The framework combines Computational Fluid Dynamics and Machine Learning based techniques, and, to the best of our knowledge, represents the first computational approach relying on 3D rotational angiography (3DRA) data for non-invasive pressure computation in CoA patients. The key features of this framework are a parameter estimation method for calibrating inlet and outlet boundary conditions, and regional mechanical wall properties, to ensure that the computational results match the patient-specific measurements, and an improved ML based pressure drop model capable of accurately determining energy losses for a wide range of flow conditions and anatomical CoA variations.

The framework is evaluated by investigating 6 patient datasets, under pre- and post-operative setting, and, since all calibration procedures converged successfully, the proposed approach is deemed robust. Comparisons were performed for the peak-to-peak and the cycle-averaged pressure drop computed using the reduced-order CFD model with that measured directly by catheter, before and after virtual and actual stenting. The mean absolute error for the peak-to-peak pressure drop, which is the most relevant measure for clinical decision making, was 3.24 mmHg for the pre- and 2.18 mmHg for the post-operative setting. Moreover, the proposed method is computationally also very efficient: the average execution time was of only 2.1 ± 0.8 minutes on a standard hardware configuration.

Finally, the 6th chapter, Discussion and Conclusions, presents the final conclusions, an overview of the original contributions, a summary of the dissemination work and future work.

2. Lattice-Boltzmann method for hemodynamics simulation

In recent years, the Lattice-Boltzmann Method has emerged as a strong alternative to traditional Finite-Element (FEM) and Finite-Difference methods (FDM) for modeling fluid flows [59, 1]. Unlike FEM based solvers, LBM does not have the need for complex meshing algorithms and operates on a Cartesian lattice, making it directly relevant to medical images. Further, the highly local structure of the LBM algorithm results in impressive performance over modern parallel architectures. Previous researches [35, 55, 37] has shown that GPU implementation of LBM can be up to 40 times faster compared to its serial counterpart depending on the flow complexity.

This chapter is structured as follows: first, a brief theoretical background of the Lattice-Boltzmann method is given, followed by a detailed description of the numerical implementation of LBM focused on performing hemodynamic computations.

2.1 Theoretical background

The Lattice-Boltzmann method (LBM) emerged from the lattice gas automata and is based on a discrete representation of the linearized Boltzmann equation on a regular Cartesian grid. Unlike the continuum Navier-Stokes based methods, that directly act on the macroscopic quantities of the flow, LBM operates at mesoscopic scale operating on the particle distribution function. Therefore, state of the fluid is described by the distribution function $f(\mathbf{x}, \mathbf{u}, t)$ where **x** is the spatial position, **u** is velocity and t is time. More specifically f is a density function indicating the probability of a particle to be located at position **x**, traveling at velocity **u** at time t.

2.1.1 Multiple relaxation time collision model

The Multiple Relaxation Time collision (MRT), also called generalized collision was first introduced by d'Humieres et. al. [16]. Its main advantage is the significantly improved stability when the viscosity approaches zero, enabling simulation of high Reynolds number flow. For MRT, the collision matrix Ω is of the form $M^{-1}SM$ where S is a diagonal matrix containing the relaxation parameters and M is an orthogonal transformation matrix that transforms the microscopic distribution functions f_i to macroscopic quantities $\mathbf{m} = M\mathbf{f}$. More specifically, the collision operation is performed in the macroscopic space, also known as moment space, rather than microscopic space. This approach enables the possibility to separate the conserved and non-conserved moments and to use separated relaxation parameter appropriately chosen for each moment i.e zero for non-conserved moments and non

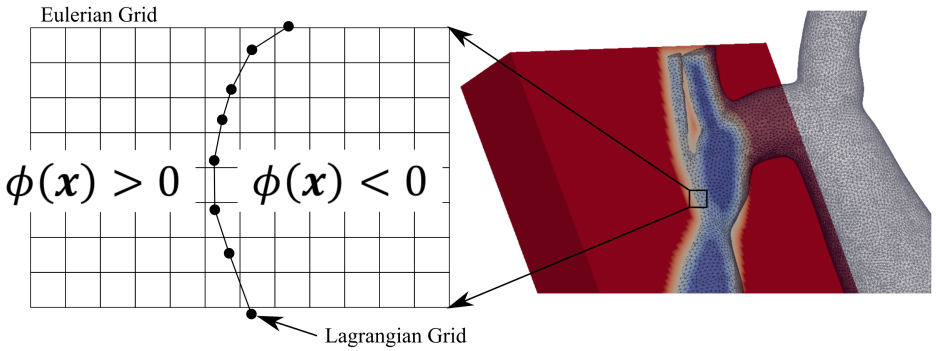

Figure 2.1: Poligonal mesh, describing the vessel surface, is embedded in the Eulerian grid through a level-set function.

zero for the rest. For example, in the work of d'Humieres et al. [16], relaxation parameters were chosen as to maximize numerical stability.

2.1.2 Entropic model

One of the most important limitations of the LBM is numerical instability that appears when viscosity is too low. Avoiding instability when simulating large Reynolds numbers using the classic LBGK or MRT collision model is possible only by using unpractically high grid resolution. Instability typically appears as a result of the distributions f_i becoming negative, therefore an approach to solve the stability issue is to formulate the collision process such that f_i are constrained to remain positive. A solution is the Entropic Lattice-Boltzmann (ELBM) [2] which is based on the Boltzmann's H theorem and it works by explicitly enforcing the second law of thermodynamics to f_i values.

2.2 Numerical implementation

This section presents some practical considerations concerning implementation of the Lattice-Boltzmann method for performing flow simulation on real patient-specific geometries. The overall workflow starts from surface meshes extracted from medical images, that describes the vessel geometry. One of the main important challenges of using LBM in this context is that LBM works on an Eulerian grid while the boundary shape (vessel geometry) is given as a polygonal mesh (Lagrangian grid). To identify the fluid and solid regions in the Eulerian grid, a voxelization operation is required which consists of transforming the given vessel surface mesh into a level-set function $\phi(\mathbf{x})$. The level-set is a scalar valued function, defined on each point $\mathbf{x}$ in the Eulerian grid and is computed such that has a negative value on the inside and positive value outside the vessel surface. A detailed description of the voxelization operation will be described in chapter 4, for now it is assumed the level-set function is computed and the problem of setting up a LBM simulation is addressed.

2.2.1 GPU acceleration

In the past, most high performance computations were executed on large clusters of computers, each capable of executing a small number of parallel threads (usually about 8 per node). However, over the last decade, general purpose Graphical Processing Units

(GPUs) have shown tremendouns increase in performance. Each GPU is capable of executing thousands of low-overhead threads simultaneously. While this kind of performance was originally developed for supporting video applications with high demands (such as gaming), they have become indispensable for scientific computing and for accelerating the performance of machine learning algorithms.

The Lattice-Boltzmann method is inherently a highly parallel algorithm, owing to the largely local nature of the computations. As discussed earlier, there are two main operations - collision and streaming. The collision step only involves computations using local information, whereas the streaming step involves communication between neighboring sets of nodes. Owing to this structure of computations, this method can exploit the advances in computing architectures such as GPUs much better than traditional techniques such as Finite-Element Methods which couple the solution at all the nodes in the domain at each time step. Indeed, there already exists a body of literature showing the high performance of LBM models which have been developed for GPU systems (for instance, [55, 37, 52, 35]).

2.3 Unit scaling and stability ranges

The Lattice-Boltzmann method presents some constraints related to the quantities involved in the simulation. More specifically LBM becomes unstable if the velocity exceeds a certain threshold and also if the viscosity gets close to zero. Therefore LBM simulations are typically preformed at a different scale rather than directly using physical quantities such that simulation remains in the stable region. This section presents the LBM specific constraints and the process of unit scaling. In the following, quantities at physical scale are written as $\mathbf{x}_{ph}$ while quantities at simulation scale are written as $\mathbf{x}_{lbm}$. Furthermore, quantites at simulation scale are considered to be non-dimensional while physical scale quantites are dimensional, therefore transforming from and to non-dimensional quantities is performed by dividing and multiplying by a reference value having the same physical units.

2.3.1 Constraints for spatial and temporal resolution

There are two constraints for quantities in LBM simulations, for velocity and viscosity. The velocity constraint exists because LBM is known to approximate the Navier-Stokes equations only for low Mach number flow, therefore velocity must be kept small such that flow remains in the low Mach number regime. It is typically argued that the non-dimensional velocity should be smaller than 0.1. As for the viscosity constraint, it is known that LBM becomes unstable as viscosity approaches zero, the threshold value depends on the chosen collision model i.e. the SRT model has the highest threshold while for the MRT model, as stability is improved, the threshold is lower. The entropic collision model is claimed to be unconditionally stable, therefore in this case there is no lower threshold for viscosity. These stability thresholds for velocity and viscosity translates eventually to some constraints that needs to be applied when choosing the spatial and temporal resolution. More specifically there is both an upper and a lower threshold for δx and δt that needs to be considered.

The two stability constraints are written as follows:

$$\nu_{lbm} > \nu_{min}, \tag{2.1}$$

$$u_{lbm} < u_{max}, \tag{2.2}$$

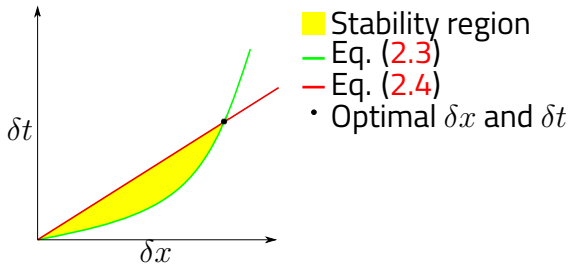

Figure 2.2: Stability region given by the LBM stability constraints: for minimum viscosity (green) and for maximum velocity (red). The optimal δx and δt values are found at the upper intersection point.

and by replacing (**??**) and (**??**) in the stability constraints yelds:

$$\nu_{ph}\frac{\delta t}{\delta x^2} > \nu_{min}, \tag{2.3}$$

$$u_{ph}\frac{\delta t}{\delta x} < u_{max}. \tag{2.4}$$

Figure 2.2 displays a graphical representation of the stability range. The optimal values are found at the upper intersection of the two curves by solving eqs. (2.3) and (2.4) for δx and δt:

$$\delta x = \frac{u_{max}}{u_{ph}}\frac{\nu_{ph}}{\nu_{lb}}, \tag{2.5}$$

$$\delta t = \frac{u_{max}^2}{u_{ph}^2}\frac{\nu_{ph}}{\nu_{lb}}. \tag{2.6}$$

Unfortunately, eqs. (2.5) and (2.6) cannot be used for computing the spatial and temporal resolution because the maximum velocity u_{max} is not known as it depends on flow conditions. In section 4.2 a detailed description on the grid resolution selection process was provided.

3. Fluid-Structure interaction simulation using Lattice-Boltzmann method

3.1 Introduction

An important component of any personalized cardiac model consists in the haemodynamics model, whose constant interaction with the cardiac walls and valves, as well as with the adjacent arteries and veins can trigger and influence various cardiac pathologies, including but not restricted to paediatric cardiomyopathy. The complexity of such a haemodynamics computation system can vary from reduced order models which lump the variables of interest (flow, pressure) in order to provide lower-dimensional descriptions, to full-scale 3D+time computational fluid dynamics models, that may include one-way or two-way interaction with the cardiac tissue and the valves.

Fluid-structure interaction simulation consists of simulating fluid flow constrained by moving boundaries. The boundaries motion can be known and directly imposed (one-way FSI) or can be computed based on the fluid forces acting on the solid (two-way FSI). For simulating arterial circulation, the solid is typically modeled as a viscoelastic material and its displacements are numerically computed using a finite element method (FEM). The other approach consists of unidirectional solid-fluid coupling where the solid displacements are known (i.e. vessel wall motions extracted from medical images) and are directly imposed to the fluid simulation.

In this chapter is presented an efficient, LBM based, method for performing fluid-structure interaction simulations for both one-way and two-way coupling. The main challenge is given by the way 3D geometry is represented. More specifically, the solid geometry is typically described as a non-uniform polygonal mesh (Lagrangian grid) while the fluid simulation is performed on an Eulerian grid. For coupling the solid and fluid simulation it is required to transfer information from the solid model (Lagrangian grid) to the Fluid model (Eulerian grid) for one-way coupling and in both directions for two-way coupling. Furthermore, this information transfer needs to be performed continuously during the simulation. Currently, this operation is a major limiting factor for performing FSI computations as it is highly computationally expensive and also it can cause numerical instability due to the explicit nature of the coupling. Therefore, optimization of this information transfer is a critical aspect.

To validate the proposed methodology, were performed various experiments using both synthetically generated and patient-specific geometries. For validating the one-way FSI simulations were performed experiments with two cases: a volume-changing vessel and three-dimensional peristaltic flow. For both of the cases there are analytical solutions available which were used to compare against the simulation results. For validating the two-way FSI simulations were performed experiments with two patient-specific cases: left ventricle

and aorta. Simulation results were then compared against velocity fields extracted from PC-MRI.

3.1.1 Image aquisition and mesh generation

The first step in the proposed FSI processing pipeline is to build the domains for both the fluid and the solid solvers. This is done by generating a patient-specific anatomical model of the vessel. To this end, 3D MRI and advanced manual or semi-automatic segmentation techniques were used to first extract an initial surface mesh of the inner surface of the patient's vessel.

So far all operations were performed on a surface mesh, i.e. a geometric structure with zero thickness. Real vessels , however, are made of several layers: tunica intima, tunica media and tunica adventitia. These layers are essentially made of cells and thus they exhibit a certain thickness , consequently the entire vessel wall has a thickness. To model this thick wall appropriately and individually for each patient, it was first created a synthetic aorta wall "hull" that is supposed to encapsulate all three layers of the vessel wall. To this end, the segmented surface mesh (inner surface) is converted into a level-set representation and the outer vessel surface is extracted from it as the iso-contour at a user-defined level set value (e.g. 1.75mm to generate a wall that is 1.75mm thick). Next, in the "tetrahedralization" step, this hull is utilized to generate a volumetric finite element mesh by filling the 3D volume encapsulated by the hull with tetrahedra, i.e. 3D cells consisting of four non-planar points. An open-source computational geometry library called CGAL [19] is used for this purpose. It is common knowledge that the aortic wall thickness can vary with age, gender, BMI, diseases, location etc. Because it can be difficult or even impossible to accurately measure aortic wall thickness from the data acquired in this project (mostly MRI) or in normal clinical routine, it was typically used a population-average value of 1.75mm as reported in literature, see e.g. [30]. The resulting finite element mesh is the computational domain for the solid (biomechanics) modelling as described in section **??**, whereas the region encapsulated by the inner surface of this mesh, i.e. the vessel lumen, is used to delineate the computational fluid domain, see chapter 2.

3.2 Moving boundaries on Eulerian grid: Solid Voxelization

Solid voxelization represents the process of transforming a polygonal mesh into a voxel representation by associating each polygon of a mesh with the cells in the voxel grid. Voxel representation of solids are currently used in many applications such as physics simulations [31], collision detection [28], volume rendering [14], etc. The main advantage of the voxel representation of a solid is that each voxel in the grid can be accessed directly by knowing its position in space or its position relative to another voxel, without performing a search operation, whereas in a mesh representation information is described sparsely as a set of polygons, by providing the position of each point explicitly. Although there are many studies on this topic, solid voxelization remains a difficult problem, mainly because of computational complexity and aspects related to robustness.

3.3 One-way fluid structure interaction

Simulating moving boundaries mainly consists of two steps: computing the surface velocity for each node on the boundary (i) and enforcing the surface velocities to the fluid. Specifically, the boundary velocity is enforced to the fluid by first computing a mapping between nodes located on the boundary mesh (Lagrangian grid) and grid nodes (Eulerian grid) that are located at the fluid-solid interface.

The boundary motion is given as a set of polygonal meshes, each describing the boundary shape at a given time. A continuous representation of the boundary motion is obtained by interpolating between the given time samples.

3.3.1 Setting moving wall velocities

When the geometry is updated, the wall velocity $\mathbf{u}_w$ is associated to each grid node close to the wall, along with the new signed distance $\phi(\mathbf{x})$. The wall velocities are enforced on the fluid boundary nodes during the streaming step. Suppose $\mathbf{x}$ is a boundary node such that $\phi(\mathbf{x}) \leq 0$ and $\phi(\mathbf{x}+\mathbf{c}_i) > 0$ where $\mathbf{c}_i$ is the current lattice direction that crosses the boundary. To treat the wall as a curved boundary it was used an interpolation scheme based on the work in [8], for which it was taken into account the exact location of the intersection point. The streaming step is performed as described in section **??** using equations (**??**) and (**??**).

3.4 One-way fluid structure interaction: Experiments

To validate the proposed methodology experiments were performed with two cases for which the analytical solution is known and can be used to compare the results. First experiment consists of a vessel that contracts and dilates through a deformation applied to the walls. Validation using this experiment consists of comparing the flow rate extracted from simulation with the exact flow rate computed from the imposed volume change. The second experiment consists of simulating three-dimensional peristaltic flow: flow through a cylindrical vessel where the walls are moved based on a wave traveling in the axial direction of the vessel. This wall movement leads to a net flow rate that can be compared with an exact solution.

3.5 Two-way fluid structure interaction

Constant interaction of the blood flow with cardiac walls, valves, and adjacent arteries and veins, can trigger and influence various cardiac pathologies. Therefore, the hemodynamics model is an important component of the proposed personalized cardiac model. The approach that it has been used so far features a limited one-way interaction with the solid parts of the simulation, as geometric changes by the cardiac walls are directly imposed on the fluid without any feed-back. The goal is to build a fluid-structure interaction (FSI) model which ties fluid and solid parts of the simulation closer together and allows bi-directional feed-back and influences. In this report, it is presented the developed methods, the updated modelling and computation pipelines, and an evaluation of the new approach in direct comparison to its one-way coupling.

Performing an FSI simulation consists of simultaneously running the fluid and solid simulations and continuously exchange information between the two. More specifically at each time step of the simulation, the following information is passed between the fluid and solid:

1. Vessel wall positions and velocities are sent from the solid to the fluid simulation. Boundaries of the fluid simulation are updated using the approach described in section 3.5.

2. Fluid wall shear stresses are sent from the fluid to the solid simulation.

3.6 Two-way fluid structure interaction: experiments

In this section, it was described the fully-coupled FSI approach and the two models that it couples. As both proposed implementations of the LBM fluid flow and the TLED solid mechanics model have already been tested extensively, but independently from one another (i.e. in their standalone versions), the focus of this report is on the fully-coupled FSI model. Therefore, in the following sections were presented a number of experiments aimed towards verifying the correctness and plausibility of the fully-coupled FSI simulation results. To demonstrate the potential of the presented methodology, two-way simulations were performed on two realistic configurations using patient-specific data extracted from MRI images: left ventricle and aorta. Furthermore it was performed an extensive validation of the model by comparing the results with flow information extracted from 4D MRI.

4. Non invasive hemodynamic assessment of cerebral aneurysms

4.1 Introduction

Intracranial aneurysms are pathological disorders which consist of an abnormal dilatation of the vessel wall. In severe cases, the aneurysm may rupture causing subarachnoid hemorrage which can lead to severe disability or death [9]. The incidence of unruptured aneurysms is high as it occurs in about 6% of the population, however rupture incidence is very low, 7.7 in 100000 cases annually [3]. Consequently, treatment of unruptured aneurysms also has a high economic cost [54]. Due to its high incidence, it is critical to accurately identify the subset of patients with high risk of rupture and plan the treatment accordingly.

There are several treatment options available to decrease the likelihood of rupture. One possibility is to surgically clip the aneurysm at its neck, to isolate the aneurysmal dome and prevent bleeding [47]. Another solution consists of filling the aneurysm with thin wires that constrict the flow and initiate a thrombotic reaction leading to a complete occlusion [33]. A recently proposed approach is based on placing a flow-diverter device that reduces the flow inside the aneurysm by directing most of the flow through the main artery and inducing intra-aneurysmal thrombosis [24, 17, 25]. To establish an accurate treatment plan and to evaluate the risk of rupture, a good understanding of the aneurysm hemodynamics is required. These can be used to predict the flow before and after implantation to investigate how much benefit is provided to the patient by different therapies.

The recent advances made in medical imaging, algorithms for automatically extracting anatomical information from the images as well as in modern computing architectures (like Graphical Processing Units), have enabled much easier workflows using physics-based computational models for patient-specific hemodynamic evaluation [45]. Blood flow computations, when used in conjunction with patient-specific anatomical models extracted from medical images, provide important insights into the structure and function of the cardiovascular system. These techniques have been proposed for diagnosis, risk stratification, and surgical planning [51].

An increasing number of researchers suggests that there is a strong link between flow related quantities and aneurysm growth or risk of rupture. This is still a highly debated subject [23, 10], and correlations found between hemodynamic quantities and aneurysm progression are not yet conclusive as researchers proposed different quantities. Boussel et al. [7] suggest that aneurysm growth occurs in regions of low wall shear stress. Takao et al. [49] evaluated energy loss, a pressure loss coefficient, wall shear stress and oscillatory shear index for the prediction of rupture in a set of 100 patients, suggesting that the pressure loss coefficient may be a potential parameter for predicting the risk of rupture.

Furthermore, there is a debate on whether low or high wall shear stress is contributing to aneurysm risk of rupture [29]. To this extent, further efforts on integrating personalized blood flow computations in clinical workflows is crucial for developing an unified theory on aneurysm pathophysiology.

There are two key problems with the large scale adoption of CFD based tools for clinical hemodynamic analysis of aneurysms. The first problem is the high demand on computational resources. CFD computations are commonly performed using an appropriate discretization of the Navier-Stokes equations using either the Finite-Element Method (FEM), Finite-Differences Methods (FDM) or Finite-Volume Methods (FVM). Models based on implicit integration using FEM have the advantage of unconditional stability along with the ability to easily adapt to complex anatomical structures, but require significant computational resources [56, 15, 34] for the solution of the resulting set of discrete equations. To further investigate the potential link between hemodynamic quantities and aneurysm outcome a large number of computations are required, hence a better performing approach for simulating blood flow on patient-specific aneurysm configuration is required. Although CFD-based approaches are nowadays routinely used in medical research activities to compute hemodynamic quantities under patient-specific conditions, the only CFD-based solution currently used in clinical practice, available only as a service, is focusing on computing fractional flow reserve in coronary arteries [36]. One of the main limitations for applying CFD solutions routinely in clinical practice is the computationally demanding aspect of these solutions. Specifically, they are not compatible with today?s clinical practice, where the cost pressure is very high, and the time a clinician can afford to dedicate to a patient is continuously decreasing.

Another significant limitation of employing CFD in clinical practice is the requirement of CFD related expertise for performing such computations e.g mesh generation, setting boundary conditions and most importantly choosing spatial and temporal resolution. Typical approaches to this problem consists of employing automated local mesh refinement techniques [34, 26, 42]. This limitation has also been addressed by Seo et. al. [44] where they proposed a solver implementation based on immersed boundary method [32] where simulations are performed on a Cartesian grid using a level-set function that is directly extracted from medical images, therefore bypassing the need of mesh generation.

To achieve a fully automated workflow for patient-specific aneurysm hemodynamics, there are two steps which need to be considered. First is the extraction of anatomical models from images and second is the flow computation. Although extracting anatomical models is a difficult problem, there are many existing solutions both fully and semi-automated [4]. The flow computation step it is considered to be still a major challenge which needs to be addressed.

Herein it was proposed an alternative approach for further automating cerebral blood flow simulations, starting from a patient-specific anatomical model reconstructed from medical images. It was used a reduced order blood flow model for computing initial estimates of the flow distribution in all the vessel branches which is then used to compute an initial grid resolution and time step. Furthermore, it was employed an iterative approach that refines the grid resolution and time step during the simulation.

To address the computational performance challenge, it was employed a Graphics Processing Unit (GPU) accelerated implementation of the Lattice-Boltzmann method (LBM). In recent years, LBM has emerged as a strong alternative to traditional Finite-Element (FEM), Finite-Difference methods (FDM) and Finite-Volume methods (FVM) for modeling fluid flows [11, 1]. Unlike FEM based solvers, LBM does not have the need for complex

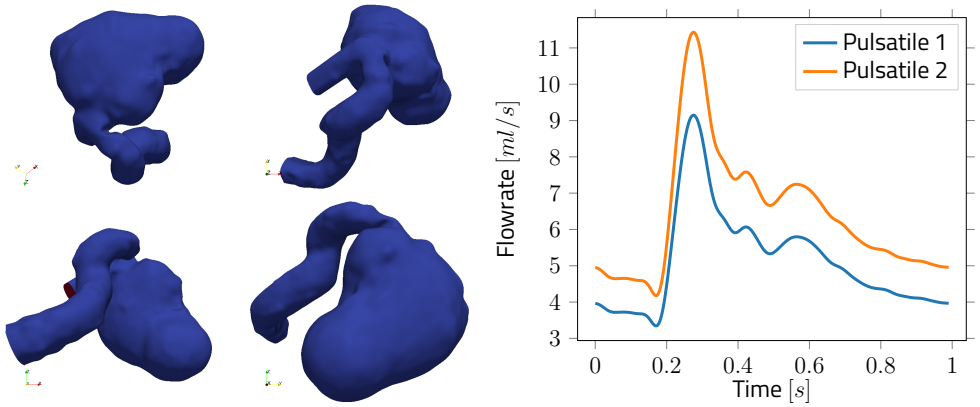

Figure 4.1: Simulation setup: the surface geometry (left), and the flow rate prescribed at the inlet boundary for the two (right).

meshing algorithms and operates on a Cartesian lattice, greatly simplifying the preprocessing step. Further, the highly local structure of the LBM algorithm results in an impressive performance on modern parallel architectures [55]. LBM has also attracted attention in the context of cerebral flow simulation: Chopard et. al. [12] employed an open source LBM implementation: Palabos [27] for studying thrombus formation in a cerebral aneurysm, Bernsdorf et. al. [6] used LBM to study flow rheology in cerebral aneurysm and Závodszky et. al. [60] performed a validation study and showed good results by comparing different LBM implementations with a finite volume solver and experimental data.

4.2 Automatic, model-based parameter selection

Reducing the user interaction and the required CFD-related expertise represents an important aspect for employing the flow solver in a clinical setting. A key feature of the implementation is the automatic tuning of the time-step δt and spatial resolution δx for optimizing accuracy and performance. To achieve this was proposed a heuristic approach based on the known LBM stability limits and some empirically chosen factors. More specifically, δt and δx are chosen to be as coarse as possible but in the same time to be small enough to capture relevant flow features and to satisfy LBM-specific stability constraints.

4.3 Verification: comparison against ASME2012 data

To evaluate the presented methodology were performed experiments on a benchmark aneurysm model previously presented in [46] as part of the "Aneurysm CFD Challange 2012" where the participants were required to perform CFD simulations and predict the flow. The case consists of a giant cerebral aneurysm with a proximal stenosis, displayed in figure 4.1. Steinman et al. [46] reported the submitted solutions and concluded that the pressure drop due to the stenosis was reasonably well predicted among the vast majority of the participants. Simulations were performed using the same configuration and compared against the solutions submitted for the challange.

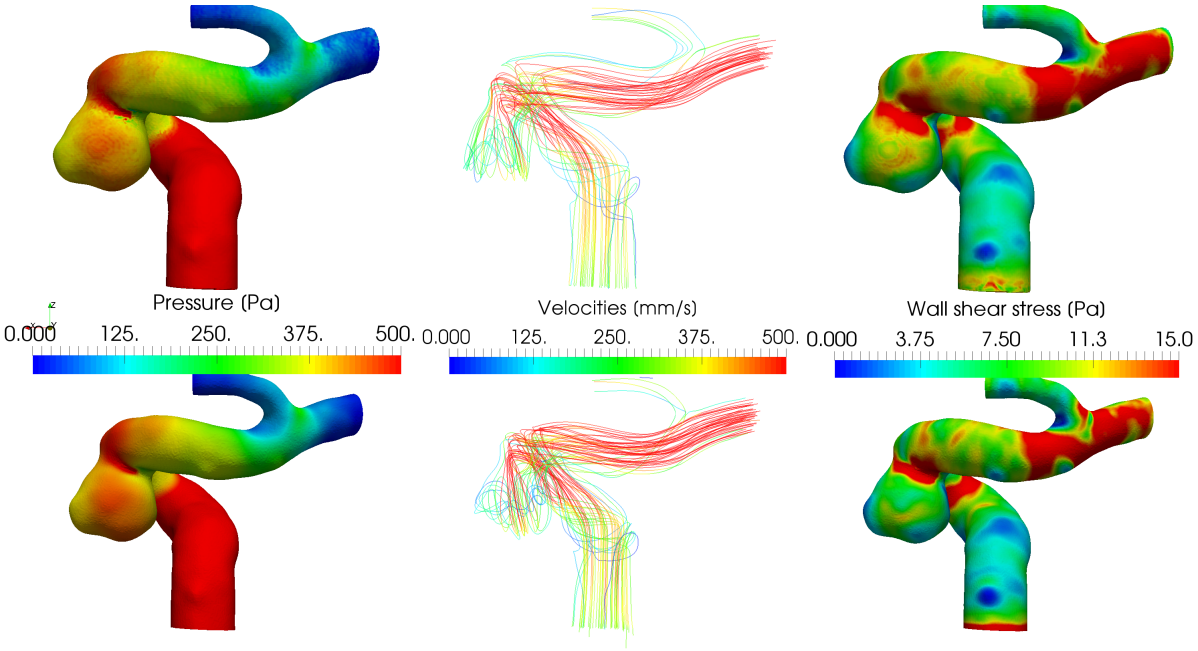

Figure 4.2: Pressures, velocities and wall shear stress for the ICA1 case at peak systole. Simulation results from LBM (first row) and Ansys CFX (second row).

4.4 Verification: comparison against a commercial solver

To further validate the solver simulations were performed on 20 patient specific aneurysm cases and compared against results obtained using a commercially available CFD solver (Ansys CFX, Canonsburg PA, www.ansys.com). The cases correspond to ten internal carotid artery (ICA) and ten middle cerebral artery (MCA) aneurysms. A more extensive verification of the solver on similar aneurysm cases was performed in [48]. Simulations were performed under the same configuration as in the previous experiments: three cardiac cycles and results were extracted from the last cycle only, at the inlet boundary a time-variable velocity is specified while the outlet is set to have zero pressure. The grid resolution was automatically estimated using the approach proposed in section 2. Figure 4.3 presents the pressure, velocity and wall shear stress (WSS) fields for both the LBM and CFX results corresponding to the ICA1 case. For all the three quantities, the LBM solutions matches well with CFX as there is no significant difference between the two solutions.

4.5 Discussion

Performing CFD computations is typically a challenging task, especially for complex flows like in cerebral aneurysms. The main challenges are given by computational complexity which leads to very large execution times, but also the requirement of an experienced user for choosing solver parameters, mesh resolution, etc. Both of these are limiting factors that severely reduces the potential of using CFD based tools in a clinical environment where computations are required to be performed on a patient basis. Herein these limitations were addressed and proposed a novel methodology for performing hemodynamics computations

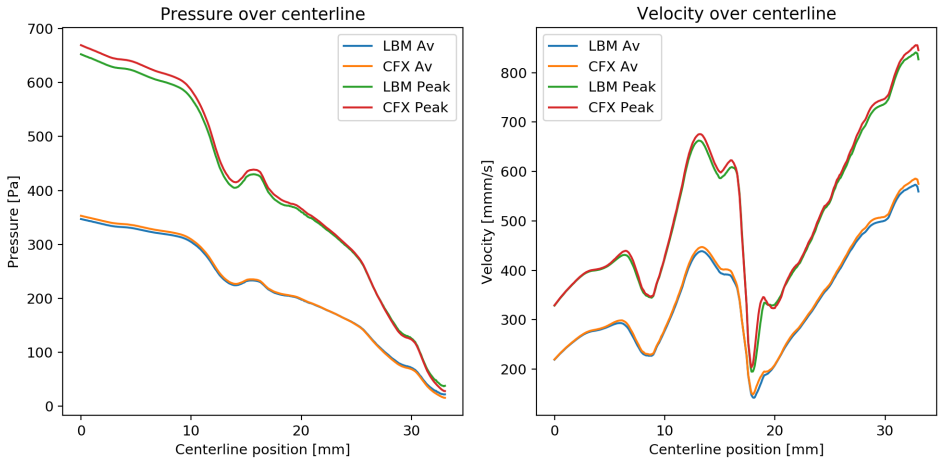

Figure 4.3: Pressures and velocities along the centerline, corresponding to the main branch of the ICA1 case.

in patient-specific cerebral aneurysms. Computational cost was significantly reduced by employing a Graphics Processing Unit implementation of the Lattice-Boltzmann Method. A CFD simulation for one cerebral aneurysm can be performed in a matter of minutes on a regular workstation compared to hours on expensive computing clusters. Computations were performed on 21 aneurysm cases and the median execution time was 40 minutes using a single commodity GPU. The measured time includes the preprocessing step, all the three cardiac cycles and also the simulation restarts required for tuning the spatial resolution and time step. Although the computation time may still be considered too high for employing such tools on a clinical setting, it can still be significantly reduced by further increasing the parallelism e.g. by using multiple GPUs simultaneously [55], as LBM is known to scale well on massively parallel hardware. Furthermore it was found that there is a strong dependence between computation time and vessel geometry complexity i.e. narrowing segments, curvature, branching, etc. As the flow develops more complex features a finer resolution is also required, therefore increasing the computation time.

5. Non invasive hemodynamic assessment of aortic coarctation

5.1 Introduction

Coarctation of the aorta (CoA) is a congenital disease that accounts for 8-11% of cardiovascular diseases [20]. It consists of a narrowing of the aortic media into the lumen of the aorta, usually located near the aortic arch, that obstructs the flow, causing a pressure drop along the narrowing, and less blood being delivered to the lower part of the body. If left untreated, it was found to cause hypertension, early coronary artery disease, heart failure, stroke, aneurysm formation and decreased life expectancy [13, 53, 39]. Treatment of CoA aims at reducing the pressure drop and restoring normal flow conditions to the lower part of the body. Treatment is typically performed surgically or percutaneously, i.e by placing a stent or by balloon angioplasty [22, 38]. In older children and particularly in teenagers and adults, catheter-based intervention is becoming more prevalent and is typically the standard of care. Although the occlusion ratio can be accurately measured from image data, e.g. MRI or trans-thoracic echocardiograply, accurate clinical decision making requires hemodynamic assessment that can be performed only invasively through pressure measurements [50]. Specifically, treatment is recommended for a resting state peak-to-peak trans-coarctation pressure drop of 20 mmHg or more [41]. The most accurate technique for measuring pressure drop is intravascular catherization.

Given the invasive nature of cardiac catheterization, and associated costs and risks, efforts have been made to develop non-invasive methods for computing the trans-CoA pressure drop from medical images. A previously reported approach consists in using flow velocity information extracted with Doppler ultrasound or phase contrast MRI (PC-MRI), in combination with fluid dynamics equations, to estimate pressure as a function of velocity [43, 57, 18]. A different approach relies on Computational Fluid Dynamics (CFD) for performing patient-specific blood flow computations. Compared to traditional techniques, the main advantage of a CFD based tool is that it offers the potential to also simulate post-treatment hemodynamics or flow under different conditions such as stress, which would normally have to be induced pharmacologically. Furthermore, CFD is able to provide quantities that are not available through measurement, e.g. Wall Shear Stress (WSS) or WSS derived quantities.

Herein, a framework was introduced for automatically and robustly personalizing aortic hemodynamic computations for the assessment of pre- and post-intervention CoA patients from 3D rotational angiography (3DRA) data. The framework combines CFD and ML based techniques for the assessment, and, to the best of our knowledge, represents the first computational approach relying on 3DRA data for non-invasive pressure computation in CoA patients. The key features of the framework are (i) a hybrid multiscale fluid-structure interac-

tion reduced-order model, (ii) a parameter estimation method for calibrating inlet and outlet boundary conditions, and regional mechanical wall properties, to ensure that the computational results match the patient-specific measurements, and (iii) an improved ML based pressure drop model capable of accurately determining energy losses for a wide range of flow conditions and anatomical CoA variations. Inspired by the original work of Young and Tsai [58], where model parameters were fitted to experimental data, the ML based pressure drop model was developed using a similar approach, but relying on in silico data. Were performed a large number of 3D CFD computations on a set of synthetically generated aortic coarctation anatomical models, and, then, trained an ML-based model for accurate CoA pressure drop prediction.

5.2 Development of a pressure-drop model tailored for aortic coarctation

It was introduced a novel analytical model for direct computation of instantaneous pressure drop in CoA segments, using aortic flow rate and relevant anatomical features of the CoA segment as input. The starting point for defining the analytical model is the previous work of Young and Tsai [58]. To further improve the accuracy of the model under pathological aortic flow conditions, were added new terms to the analytical expression, and adapt all parameters by performing a machine learning based optimization on a large database of three-dimensional (3D) CFD computation results generated for synthetic CoA anatomical models. To generate the synthetic anatomical models were used previously reconstructed patient-specific CoA anatomical models as starting point [40]. Thus, 200 synthetic anatomical models were generated, and multiple computations were run for each anatomical model, using different inlet flow rates as described below. The pressures extracted from the 3D CFD computations were then employed to calibrate the model parameters.

5.3 Results

5.3.1 Evaluation of the pressure drop model

First it was evaluated the performance of the optimized and the original Young-Tsai model using the 3D CFD computations as ground truth: figure 5.1 displays the results on the test set.

5.4 Discussion and conclusions

A key ingredient of the proposed solution is the development of a coarctation specific machine learning based pressure drop model. A comprehensive training database is an important prerequisite for the successful development of such a model. In an ideal scenario, the training database would consist of thousands of anatomical models extracted from medical images, accounting for the variability of aortic coarctations across different patient populations, and the corresponding invasive pressure measurements of each narrowing. From a practical point-of-view, establishing such a large database would be prohibitively expensive and time-consuming.

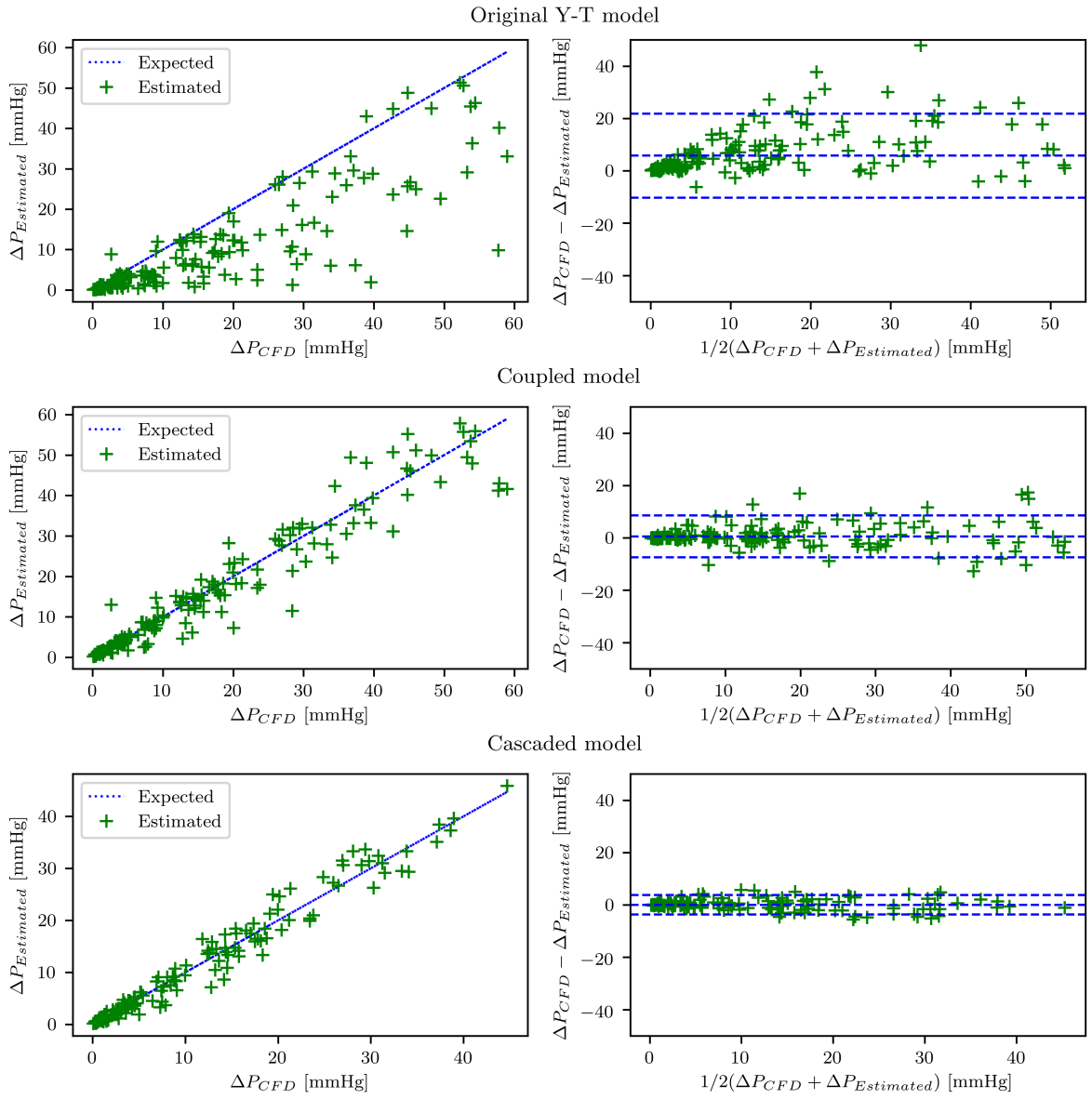

Figure 5.1: Evaluation of the pressure drop models. ΔP_{CFD} represents the pressure drop extracted from the 3D CFD computations, while $\Delta P_{Estimated}$ is the pressure drop determined analytically using the pressure drop models: top - original Young-Tsai model (equation (**??**)), middle - optimized pressure drop model and bottom - coupled model.

The ability to have predictive modeling with hemodynamic assessment in the cardiac catheterization laboratory will allow for clinical decisions regarding stent therapy to be based on robust data. This has the ability to revolutionize the way clinical decisions are made and to improve patient care significantly. Moreover, the proposed methodology is complementary with respect to previously introduced CFD based approaches relying on MRI / CT data, which may be employed to avoid invasive catheterization for patients with functionally non-significant CoA.

6. Final conclusions

6.1 Conclusions

The main focus of the present work was to develop and evaluate numerical methods for performing blood flow computations under patient specific conditions with the purpose of providing insight into the cardiovascular system and specific cardiovascular diseases. The work was mainly focused on performing three-dimensional flow simulations in multiple variations and for different scenarios. Although CFD is a mature field with many existing and verified tools for performing such computations, employing it for the cardiovascular system is a challenging task. First of all, the cardiovascular system is a very complex and highly coupled system involving many processes which take place at different scales. Unfortunately, standard CFD alone is not sufficient for capturing enough complexity in most cases and coupling with other methods is required. Another important challenge is computational performance. It is known that CFD is a very demanding process in terms of computing power and time, however, for most use cases outside the medical field, this is not a severe limitation. Employing such tools in the medical field requires simulations to be performed in a patient-specific manner, which means a high number of CFD simulations are required. This turns the computational cost into one of the most significant limitations.

To this extent, the main focus of this work lied on the LBM method as a strong alternative to standard CFD methods. Thanks to its formulation, LBM was found to be well suited for blood flow computations with a series of advantages. First, the LBM implementation is inherently parallel and was shown to perform very well on GPU hardware. If properly implemented by carefully considering constraints related to the architecture of a GPU, the resulting performance can be unprecedently high. Although there are many studies proposing GPU based implementations of LBM and reporting great performance, there are very few studies where such computations were performed on real patient-specific anatomies and with parameters chosen in physiological ranges. Another significant advantage of LBM compared to classic, continuum-based methods is the ability to handle complex geometries without requiring a meshing operation. Since the LBM implementation works on a Cartesian grid, defining a complex fluid domain can be simply done by marking locations in the grid as being solid or fluid. This feature was shown to also be well suited for FSI simulations where fluid boundaries are moving. More specifically, the motion of the boundary can be very simply prescribed by just changing grid locations from fluid to solid or vice-versa. This is a very complex operation when classic, e.g. FEM-based methods, are employed. In these cases, updating the fluid domain requires the corresponding mesh to be updated. In turn, this update operation also requires the mesh to be regenerated at certain locations for preventing it from becoming degenerated.

The next scenario considered in this work was the coupling of LBM with other methodologies for including the effect of other physical processes involving blood flow. The most

significant process to be considered was the interaction with vessel walls. Blood vessels are made of elastic tissue that can expand and contract depending on the blood pressure and many other factors like the surroundingtissue. Performing a fluid-solid coupled simulation requires two simulations to be run separately for the fluid and solid components, as there is no unified mathematical model for both. This separation also implies that information needs to be exchanged explicitly between the two components, and at very high frequency. More specifically, in the case of fluid-solid coupling, the solid is moved by the fluid pressure while the fluid is driven by the solid displacement. This bidirectional exchange results in a coupled system where both the fluid and the solid are affected by each other. A simpler case is when this coupling is performed only in one direction: solid motion is known and is imposed at the fluid boundary. Both of these cases were addressed in the current work and a series of methodologies were proposed for performing such computations with LBM. The main limitation for performing FSI computations on patient-specific anatomies is the very high computation time. Although the GPU-LBM based flow simulation is very fast, coupling it with the solid simulation limits the computational performance significantly. This is mostly due to how the information is exchanged between the two simulations: the fluid simulation is performed with LBM on a Cartesian grid, while the solid simulation is performed with a standard FEM method on an irregular mesh. Therefore, for exchanging nodal information between these two simulations, it is required for the data to be interpolated on each grid. Unfortunately, this is not a straightforward operation because it requires the algorithm to search for the closest node on the irregular mesh, and this search operation would be required for each boundary node. To address this limitation an optimized method was proposed which is based on heuristics for removing the need for a search operation. Furthermore, it was shown that the proposed method is highly parallel and can benefit from the GPU architecture. Finally, it was shown that the total computational time overhead of FSI compared to a regular flow simulation can be reduced to only 50%.

Finally, to evaluate the results of the proposed methods, a series of experiments on real patient-specific data were performed. Two scenarios were considered: left ventricle and aorta. Both two-way and one-way simulations were performed with these cases. The results were evaluated by comparing them with flow velocities extracted from 4D MRI data acquired from the same patients. Although 4D MRI is able to provide accurate measurements for velocity fields, using these as reference data for validating the simulations was not straightforward because of the inherent noise in the data. To address this limitation a segment-wise averaged comparison was performed, indicating a good agreement between computations and measurements.

The second major goal of the present work was to advance the proposed methods towards clinical routine use by evaluating their potential to be used in non-invasive diagnosis workflows. To achieve this, two specific scenarios were considered: cerebral aneurysms and aortic coarctation. For both of these pathologies it was previously shown that flow related characteristics are playing an important role. For both cases a first step was to validate the simulation results with existing reference data. For aneurysmal flow it is currently not possible to perform an in-vivo validation as there is no way of performing any relevant measurements on a patient. To overcome this limitation, the validation study was conducted by comparing results with existing reference data reported in literature and with a mature, state-of-the-art, commercially available CFD solver (Ansys CFX, Canonsburg PA). The comparison against the commercial solver was based on 20 patient-specific anatomies extracted from MRI images. The comparison showed exceptionally good agreement between results, with an average error of 2% for velocity and pressure. A GPU-accelerated imple-

mentation was proposed along with a series of optimizations, resulting in a median execution time of 40 minutes per patient. Although this can be considered still to high for an application in a clinical setting, the run-time performance is still orders of magnitude better compared to reference metrics from literature.

The last scenario that was addressed is the non-invasive hemodynamic assessment of aortic coarctation. Aortic coarctation is a congenital disease which consists on a narrowing of the aorta which restricts blood flow to lower part of the body. An important parameter for evaluaring the severity of the coarctation, and, hence, for its diagnosis is the pressure drop across the narrowed aortic segment. This pressure drop is typically measured invasively using a catheter, which is a costly procedure bearing certain risks for the patient. Therefore, a non-invasive approach of estimating the pressure drop can be considered extremely valuable for diagnosing aortic coarctation patients. To this extent, was evaluated the potential of using CFD computations of the aortic flow for estimating the pressure drop. This, however was found to be a difficult task to achieve. Compared to other regions of the cardiovascular system, the aortic flow is a very complex mainly because of the very high Reynolds number. To simulate such complex flow a very fine spatial and temporal resolution is required which causes the run-time performance to be very low. A first attempt to address this limitation was to employ turbulence models which allows simulation to be run with coarser resolution. However it was found that the resulting run-times weren't sufficiently small for employing such computations in a clinical workflow. Therefore, a completely different approach was considered: instead of performing full-scale CFD simulations, a statistical model was developed. The main reasoning behind this approach was that only the pressure drop across the coarctation region is needed, hence it is not necessary to perform an entire three-dimensional CFD simulation. To this extent a statistical model was developed which consists from a coupled machine learning and physiologically inspired component. The model was tuned by performing a large number of three-dimensional CFD simulations of the aorta on realistic synthetically generated aortic vessels. Then, the model was trained to predict the pressure based on the resulting database of simulations and associated geometric parameters. Finally the pressure model was evaluated based on both CFD and real invasively measured pressures, resulting in a relative error of only 1%.

Bibliography

[1] C. K. Aidun and J. R. Clausen. Lattice-boltzmann method for complex flows. Annual Review of Fluid Mechanics, 42:439–472, 2010.

[2] S. Ansumali, I. V. Karlin, and H. C. Öttinger. Minimal entropic kinetic models for hydrodynamics. EPL (Europhysics Letters), 63(6):798, 2003.

[3] G. Asaithambi, M. M. Adil, S. A. Chaudhry, and A. I. Qureshi. Incidences of unruptured intracranial aneurysms and subarachnoid hemorrhage: results of a statewide study. Journal of vascular and interventional neurology, 7(3):14, 2014.

[4] M. A. Balafar, A. R. Ramli, M. I. Saripan, and S. Mashohor. Review of brain mri image segmentation methods. Artificial Intelligence Review, 33(3):261–274, 2010.

[5] E. J. Benjamin, M. J. Blaha, S. E. Chiuve, M. Cushman, S. R. Das, R. Deo, J. Floyd, M. Fornage, C. Gillespie, C. Isasi, et al. Heart disease and stroke statistics-2017 update: a report from the american heart association. Circulation, 135(10):e146–e603, 2017.

[6] J. Bernsdorf and D. Wang. Blood flow simulation in cerebral aneurysm: A lattice boltzmann application in medical physics. In Parallel Computational Fluid Dynamics 2007, pages 291–296. Springer, 2009.

[7] L. Boussel, V. Rayz, C. McCulloch, A. Martin, G. Acevedo-Bolton, M. Lawton, R. Higashida, W. S. Smith, W. L. Young, and D. Saloner. Aneurysm growth occurs at region of low wall shear stress patient-specific correlation of hemodynamics and growth in a longitudinal study. Stroke, 39(11):2997–3002, 2008.

[8] M. Bouzidi, M. Firdaouss, and P. Lallemand. Momentum transfer of a boltzmann-lattice fluid with boundaries. Physics of fluids, 13(11):3452–3459, 2001.

[9] J. L. Brisman, J. K. Song, and D. W. Newell. Cerebral aneurysms. New England Journal of Medicine, 355(9):928–939, 2006.

[10] J. R. Cebral and H. Meng. Counterpoint: realizing the clinical utility of computational fluid dynamics—closing the gap, 2012.

[11] S. Chen and G. D. Doolen. Lattice boltzmann method for fluid flows. Annual review of fluid mechanics, 30(1):329–364, 1998.

[12] B. Chopard, D. Lagrava, O. Malaspinas, R. Ouared, J. Latt, K.-O. Lovblad, and V. Pereira-Mendes. A lattice boltzmann modeling of bloodflow in cerebral aneurysms. In V Eur Conf Comput Fluid Dyn ECCOMAS CFD, volume 453, page 12, 2010.

[13] M. Cohen, V. Fuster, P. M. Steele, D. Driscoll, and D. C. Mcgoon. Coarctation of the aorta. long-term follow-up and prediction of outcome after surgical correction. Circulation, 80(4):840–845, 1989.

[14] C. Crassin, F. Neyret, S. Lefebvre, and E. Eisemann. Gigavoxels: Ray-guided streaming for efficient and detailed voxel rendering. In Proceedings of the 2009 symposium on Interactive 3D graphics and games, pages 15–22. ACM, 2009.

[15] K. D. Dennis, D. F. Kallmes, and D. Dragomir-Daescu. Cerebral aneurysm blood flow simulations are sensitive to basic solver settings. Journal of Biomechanics, 57:46–53, 2017.

[16] D. d'Humières. Multiple–relaxation–time lattice boltzmann models in three dimensions. Philosophical Transactions of the Royal Society of London A: Mathematical, Physical and Engineering Sciences, 360(1792):437–451, 2002.

[17] P. I. D'Urso, G. Lanzino, H. J. Cloft, and D. F. Kallmes. Flow diversion for intracranial aneurysms a review. Stroke, 42(8):2363–2368, 2011.

[18] T. Ebbers, L. Wigström, A. F. Bolger, J. Engvall, and M. Karlsson. Estimation of relative cardiovascular pressures using time-resolved three-dimensional phase contrast mri. Magnetic resonance in medicine, 45(5):872–879, 2001.

[19] A. Fabri and S. Pion. Cgal: The computational geometry algorithms library. In Proceedings of the 17th ACM SIGSPATIAL international conference on advances in geographic information systems, pages 538–539. ACM, 2009.

[20] C. Ferencz, J. D. Rubin, R. J. Mccarter, J. I. Brenner, C. A. Neill, L. W. Perry, S. I. Hepner, and J. W. Downing. Congenital heart disease: prevalence at livebirth: the baltimore-washington infant study. American journal of epidemiology, 121(1):31–36, 1985.

[21] X. He and L.-S. Luo. Lattice boltzmann model for the incompressible navier–stokes equation. Journal of statistical Physics, 88(3-4):927–944, 1997.

[22] W. E. Hellenbrand, H. D. Allen, R. J. Golinko, D. J. Hagler, W. Lutin, and J. Kan. Balloon angioplasty for aortic recoarctation: results of valvuloplasty and angioplasty of congenital anomalies registry. The American journal of cardiology, 65(11):793–797, 1990.

[23] D. F. Kallmes. Point: Cfd-computational fluid dynamics or confounding factor dissemination. American Journal of Neuroradiology, 33(3):395–396, 2012.

[24] C. Karmonik, J. Anderson, J. Beilner, J. Ge, S. Partovi, R. P. Klucznik, O. Diaz, Y. Zhang, G. W. Britz, R. Grossman, et al. Relationships and redundancies of selected hemodynamic and structural parameters for characterizing virtual treatment of cerebral aneurysms with flow diverter devices. Journal of biomechanics, 49(11):2112–2117, 2016.

[25] Y. H. Kim, X. Xu, and J. S. Lee. The effect of stent porosity and strut shape on saccular aneurysm and its numerical analysis with lattice boltzmann method. Annals of biomedical engineering, 38(7):2274–2292, 2010.

[26] D. Lagrava, O. Malaspinas, J. Latt, and B. Chopard. Automatic grid refinement criterion for lattice boltzmann method. arXiv preprint arXiv:1507.06767, 2015.

[27] J. Latt. Palabos, parallel lattice boltzmann solver, 2009.

[28] O. S. Lawlor and L. V. Kalée. A voxel-based parallel collision detection algorithm. In Proceedings of the 16th international conference on Supercomputing, pages 285–293. ACM, 2002.

[29] H. Meng, V. Tutino, J. Xiang, and A. Siddiqui. High wss or low wss? complex interactions of hemodynamics with intracranial aneurysm initiation, growth, and rupture: toward a unifying hypothesis. American Journal of Neuroradiology, 35(7):1254–1262, 2014.

[30] B. Mensel, J.-P. Kühn, T. Schneider, A. Quadrat, and K. Hegenscheid. Mean thoracic aortic wall thickness determination by cine mri with steady-state free precession: validation with dark blood imaging. Academic radiology, 20(8):1004–1008, 2013.

[31] V. Mihalef, D. Metaxas, M. Sussman, V. Hurmusiadis, and L. Axel. Atrioventricular blood flow simulation based on patient-specific data. Functional Imaging and modeling of the heart, pages 386–395, 2009.

[32] R. Mittal and G. Iaccarino. Immersed boundary methods. Annu. Rev. Fluid Mech., 37:239–261, 2005.

[33] Y. Murayama, Y. L. Nien, G. Duckwiler, Y. P. Gobin, R. Jahan, J. Frazee, N. Martin, and F. Viñuela. Guglielmi detachable coil embolization of cerebral aneurysms: 11 years' experience. Journal of neurosurgery, 98(5):959–966, 2003.

[34] F. Mut, R. Aubry, R. Löhner, and J. R. Cebral. Fast numerical solutions of @articlebotti2010adaptive, title=An adaptive mesh refinement solver for large-scale simulation of biological flows, author=Botti, Lorenzo and Piccinelli, Marina and Ene-Iordache, Bogdan and Remuzzi, Andrea and Antiga, Luca, journal=International Journal for Numerical Methods in Biomedical Engineering, volume=26, number=1, pages=86–100, year=2010, publisher=Wiley Online Library @articlelagrava2015automatic, title=Automatic grid refinement criterion for lattice Boltzmann method, author=Lagrava, Daniel and Malaspinas, Orestis and Latt, Jonas and Chopard, Bastien, journal=arXiv preprint arXiv:1507.06767, year=2015 patient-specific blood flows in 3d arterial systems. International journal for numerical methods in biomedical engineering, 26(1):73–85, 2010.

[35] C. Nita, L. M. Itu, and C. Suciu. Gpu accelerated blood flow computation using the lattice boltzmann method. In High Performance Extreme Computing Conference (HPEC), 2013 IEEE, pages 1–6. IEEE, 2013.

[36] B. L. Nørgaard, J. Leipsic, S. Gaur, S. Seneviratne, B. S. Ko, H. Ito, J. M. Jensen, L. Mauri, B. De Bruyne, H. Bezerra, et al. Diagnostic performance of noninvasive fractional flow reserve derived from coronary computed tomography angiography in suspected coronary artery disease: the nxt trial (analysis of coronary blood flow using ct angiography: Next steps). Journal of the American College of Cardiology, 63(12):1145–1155, 2014.

[37] C. Obrecht, F. Kuznik, B. Tourancheau, and J.-J. Roux. Multi-gpu implementation of the lattice boltzmann method. Computers & Mathematics with Applications, 65(2):252–261, 2013.

[38] C. Ovaert, L. Benson, D. Nykanen, and R. Freedom. Transcatheter treatment of coarctation of the aorta: a review. Pediatric cardiology, 19(1):27–44, 1998.

[39] R. Puranik, V. T. Tsang, S. Puranik, R. Jones, S. Cullen, P. Bonhoeffer, M. L. Hughes, and A. M. Taylor. Late magnetic resonance surveillance of repaired coarctation of the aorta. European Journal of Cardio-Thoracic Surgery, 36(1):91–95, 2009.

[40] K. Ralovich, L. Itu, D. Vitanovski, P. Sharma, R. Ionasec, V. Mihalef, W. Krawtschuk, Y. Zheng, A. Everett, G. Pongiglione, et al. Noninvasive hemodynamic assessment, treatment outcome prediction and follow-up of aortic coarctation from mr imaging. Medical physics, 42(5):2143–2156, 2015.

[41] E. Rosenthal. Stent implantation for aortic coarctation: the treatment of choice in adults?, 2001.

[42] F. Schornbaum and U. Rüde. Massively parallel algorithms for the lattice boltzmann method on nonuniform grids. SIAM Journal on Scientific Computing, 38(2):C96–C126, 2016.

[43] B. L. Seifert, K. DesRochers, M. Ta, G. Giraud, M. Zarandi, M. Gharib, and D. J. Sahn. Accuracy of doppler methods for estimating peak-to-peak and peak instantaneous gradients across coarctation of the aorta: an in vitro study. Journal of the American Society of Echocardiography, 12(9):744–753, 1999.

[44] J.-H. Seo, P. Eslami, J. Caplan, R. J. Tamargo, and R. Mittal. A highly automated computational method for modeling of intracranial aneurysm hemodynamics. Frontiers in physiology, 9, 2018.

[45] D. A. Steinman. Image-based computational fluid dynamics modeling in realistic arterial geometries. Annals of biomedical engineering, 30(4):483–497, 2002.

[46] D. A. Steinman, Y. Hoi, P. Fahy, L. Morris, M. T. Walsh, N. Aristokleous, A. S. Anayiotos, Y. Papaharilaou, A. Arzani, S. C. Shadden, et al. Variability of computational fluid dynamics solutions for pressure and flow in a giant aneurysm: the asme 2012 summer bioengineering conference cfd challenge. Journal of biomechanical engineering, 135(2):021016, 2013.

[47] D. A. Steven. Outcome of surgical clipping of unruptured aneurysms as it compares with a 10-year nonclipping survival period. Neurosurgery, 60(1):E208, 2007.

[48] T. Suzuki, C. I. Nita, S. Rapaka, H. Takao, V. Mihalef, S. Fujimura, C. Dahmani, P. Sharma, H. Mamori, T. Ishibashi, et al. Verification of a research prototype for hemodynamic analysis of cerebral aneurysms. In Engineering in Medicine and Biology Society (EMBC), 2016 IEEE 38th Annual International Conference of the, pages 2921–2924. IEEE, 2016.

[49] H. Takao, Y. Murayama, S. Otsuka, Y. Qian, A. Mohamed, S. Masuda, M. Yamamoto, and T. Abe. Hemodynamic differences between unruptured and ruptured intracranial aneurysms during observation. Stroke, 43(5):1436–1439, 2012.

[50] D. Tanous, L. N. Benson, and E. M. Horlick. Coarctation of the aorta: evaluation and management. Current opinion in cardiology, 24(6):509–515, 2009.

[51] C. A. Taylor and D. A. Steinman. Image-based modeling of blood flow and vessel wall dynamics: applications, methods and future directions. Annals of biomedical engineering, 38(3):1188–1203, 2010.

[52] J. Tölke. Implementation of a lattice boltzmann kernel using the compute unified device architecture developed by nvidia. computing and Visualization in Science, 13(1):29–39, 2010.

[53] G. Webb. Treatment of coarctation and late complications in the adult. In Seminars in thoracic and cardiovascular surgery, volume 17, pages 139–142. Elsevier, 2005.

[54] D. O. Wiebers, J. C. Torner, and I. Meissner. Impact of unruptured intracranial aneurysms on public health in the united states. Stroke, 23(10):1416–1419, 1992.

[55] W. Xian and A. Takayuki. Multi-gpu performance of incompressible flow computation by lattice boltzmann method on gpu cluster. Parallel Computing, 37(9):521–535, 2011.

[56] L. Xu, L. Gu, and H. Liu. Exploring potential association between flow instability and rupture in patients with matched-pairs of ruptured–unruptured intracranial aneurysms. BioMedical Engineering OnLine, 15(2):461, 2016.

[57] G.-Z. Yang, P. J. Kilner, N. B. Wood, S. R. Underwood, and D. N. Firmin. Computation of flow pressure fields from magnetic resonance velocity mapping. Magnetic resonance in medicine, 36(4):520–526, 1996.

[58] D. F. Young and F. Y. Tsai. Flow characteristics in models of arterial stenoses-i. steady flow. Journal of biomechanics, 6(4):395–402, 1973.

[59] D. Yu, R. Mei, L.-S. Luo, and W. Shyy. Viscous flow computations with the method of lattice boltzmann equation. Progress in Aerospace Sciences, 39(5):329–367, 2003.

[60] G. Závodszky and G. Paál. Validation of a lattice boltzmann method implementation for a 3d transient fluid flow in an intracranial aneurysm geometry. International Journal of Heat and Fluid Flow, 44:276–283, 2013.

Abstract

Progress in recent years in medical imaging and 3D segmentation and reconstruction techniques has enabled the development of methods for non-invasive analysis of the human circulatory system. Despite progress in this area, diagnosis of cardiovascular diseases remains a difficult task, and invasive measurements that may pose certain risks are often required. As a result, a major interest has emerged in the use of non-invasive diagnostic techniques based on images and numerical methods. In this work the issue of using three-dimensional fluid simulations for the non-invasive diagnosis of cardiovascular system pathologies was studied. Although such simulation methods have been used in other areas for many years, their use in the medical context is subject to constraints. Two main objectives have therefore been considered: To develop coupled methods to simulate hemodynamic and fluid-solid interaction under different conditions (I) and to improve the potential for using these methods in a clinical environment for the non-invasive diagnosis of cardiovascular diseases (II). For the first objective a number of methods have been proposed that allow for the efficient simulation of hemodynamics in several scenarios: coupled simulation of the fluid-solid interaction, various coupling strategies and performance improvement considerations. For the 2nd objective, a number of experiments have been carried out to demonstrate the potential of their use in a clinical environment as reliable tools. Experiments with real data, obtained from medical images, and validation studies have been performed that demonstrate the accuracy of the obtained results.

Rezumat

Progresele înregistrate în ultimii ani în domeniul imagisticii medicale cât și în ceea ce privesc tehnicile de segmentare și de reconstrucție 3D au permis dezvoltarea unor metode de analiză non-invazivă a sistemului circulator uman. În pofida progreselor realizate în domeniul menționat, diagnosticarea bolilor cardiovasculare rămâne o sarcină dificilă, de cele mai multe ori fiind necesare măsurători invazive ce prezinta anumite riscuri. Ca urmare, a apărut un interes major pentru utilizarea unor tehnici de diagnosticare non-invazivă, bazate pe imagini și metode numerice. În această lucrare a fost studiată problema utilizării simulărilor de fluide tri-dimensionale în diagnosticarea non-invazivă a unor patologii ale sistemului cardiovascular. Cu toate că astfel de metode de simulare sunt folosite de mulți ani în alte domenii, utilizarea lor în contextul medical este supusă unor constrângeri. Prin urmare, s-au avut în vedere două obiective principale: dezvoltarea unor metode cuplate ce permit simularea hemodinamicii și a interacțiunii fluid-solid în diferite condiții (I) și îmbunătățirea potențialului de utilizare a acestor metode într-un mediu clinic pentru diagnosticarea neinvazivă a unor patologii cardiovasculare (II). Pentru primul obiectiv au fost propuse o serie de metode ce permit simularea eficientă a hemodinamicii în mai multe scenarii: simularea cuplată a interacțiunii fluid-solid, diverse strategii de cuplare și considerente pentru îmbunătățirea performanței. Pentru al 2-lea obiectiv au fost efectuate o serie de experimente pentru a demonstra potențialul utilizării lor într-un mediu clinic ca metode verificate si de încredere. Au fost efectuate experimente cu date reale, extrase din imagini medicale și studii de validare a rezultatelor ce demonstrează precizia rezultatelor obținute.